SiGe growth on patterned Si(001) substrates: Surface evolution and evidence of modified island coarsening

J. J. Zhang[a] and M. Stoffel
Max-Planck-Institut für Festkörperforschung, Heisenbergstraße 1, D-70569 Stuttgart, Germany

A. Rastelli and O. G. Schmidt
Max-Planck-Institut für Festkörperforschung, Heisenbergstraße 1, D-70569 Stuttgart, Germany and Institute for Integrative Nanosciences, IFW Dresden, Helmholtzstrasse 20, D-01069 Dresden, Germany

V. Jovanović and L. K. Nanver
Laboratory of Electronic Components Technology and Materials, DIMES, Delft University of Technology, 2628 CT Delft, The Netherlands

G. Bauer
Institut für Halbleiter und Festkörperphysik, Johannes Kepler Universität, A-4040 Linz, Austria

(Received 8 July 2007; accepted 5 October 2007; published online 24 October 2007)

The morphological evolution of both pits and SiGe islands on patterned Si(001) substrates is investigated. With increasing Si buffer layer thickness the patterned holes transform into multifaceted pits before evolving into inverted truncated pyramids. SiGe island formation and evolution are studied by systematically varying the Ge coverage and pit spacing and quantitative data on the influence of the pattern periodicity on the SiGe island volume are presented. The presence of pits allows the fabrication of uniform island arrays with any of their equilibrium shapes. © *2007 American Institute of Physics*. [DOI: 10.1063/1.2802555]

Strain driven self-assembly of semiconductor three-dimensional (3D) islands or "quantum dots" has been a field of intense research during the last years.[1] Among the different strained material combinations investigated so far, the Ge/Si(001) system is often considered as a prototype for understanding fundamental properties of heteroepitaxial growth. After completion of a 3–4 ML thick wetting layer (WL), 3D islands form and they evolve from rough, unfaceted prepyramids to truncated pyramids (TPs), pyramids (Ps), transitional domes (TDs), domes (Ds), and eventually steeper barns (Bs) before plastic relaxation occurs.[2] If the growth is performed on planar substrates, the islands form randomly. For their integration in novel device architectures such as dot based field effect transistors,[3–5] perfectly ordered SiGe island arrays are required to allow their external addressability. For this purpose new approaches were developed based on a combination of lithography and self-organized growth.[6] Long range ordering in two dimensions using either selective epitaxial growth through oxide masks[7] or direct growth on prepatterned substrates[8–10] was successfully demonstrated and excellent size homogeneities were reported.[11] However, the island formation and subsequent evolution on pit-patterned Si(001) substrates are still not completely understood. While the initial stages of the two-dimensional (2D) to 3D transition during Ge deposition on a pit-patterned Si(001) surface have been recently studied,[12] a detailed investigation of the morphological changes occurring during island growth is still lacking.

In this letter, we investigate the morphological evolution of the pit-patterned Si(001) surface during buffer growth and the SiGe island shape changes during subsequent Ge deposition. During Si buffer growth, the initially circular holes evolve first into multifaceted pits and eventually into inverted truncated pyramids. The Ge coverage variation allows us to follow the SiGe island shape changes occurring during growth and to highlight substantial differences with respect to the growth on planar substrates. On planar substrates islands generally have a multimodal shape distribution[13] and monomodal shape distributions are obtained only under particular growth conditions.[14–16] In contrast, growth on patterned substrates allows us to obtain homogeneous arrays consisting of any of the equilibrium shapes simply by varying the deposited amount of Ge. This indicates that growth on hole-patterned substrates is a viable path to achieve not only spatially but also morphologically ordered island ensembles.

2D arrays of holes were patterned into 4 in. Si(001) wafers by optical lithography and reactive ion etching. Each wafer consists of 54 dies and each die contains four patterned fields with size of 1.5×1.5 mm^2 with periods of 600, 800, 900, and 1000 nm. After cutting the wafer into 9.0×9.0 mm^2 dies and *ex situ* chemical cleaning, the samples were dipped in a diluted HF solution. After *in situ* outgassing at 620 °C, the substrate temperature was decreased to 360 °C and a Si buffer layer was deposited at a rate of 0.06 nm/s using solid source molecular beam epitaxy while ramping the substrate temperature from 360 to 500 °C. After Si buffer growth, the temperature was ramped up to 700 °C at a rate of 1 °C/s before either cooling down to room temperature to observe the morphology of the pits or initiating Ge deposition at a rate of 0.04 ML/s to form SiGe islands. The surface morphology was investigated using atomic force microscopy (AFM) operating in tapping mode.

Figure 1 shows AFM scans of the patterned Si(001) substrates taken before [Fig. 1(a)] and after deposition of different Si buffer layer thicknesses [Figs. 1(b)–1(d)]. After patterning, a 2D array of pits is obtained [Fig. 1(a)]. They are circular and have an average depth and diameter of about 80 and 300 nm, respectively. After depositing a 36 nm thick Si

[a]Author to whom correspondence should be addressed; also at Institut für Halbleiter und Festkörperphysik, Johannes Kepler Universität, A-4040 Linz, Austria; electronic mail: jianjun.zhang@jku.at

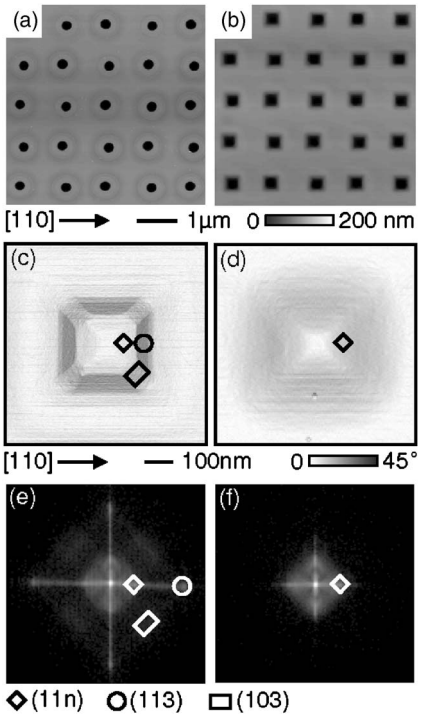

FIG. 1. AFM scans of patterned Si(001) substrates taken before (a) and after deposition of a 36 nm thick Si buffer (b). AFM scans of single pits after deposition of 72 nm Si (c) and 144 nm Si (d). Shading allows shallow and steep facets to be distinguished according to the local surface slope with respect to the (001) plane. The corresponding facet plots are shown in (e) and (f).

buffer [Fig. 1(b)], the circular pits evolve into square based morphologies having edges aligned along the ⟨110⟩ directions. Their depth decreases by about 20 nm while their diameter increases by about 200 nm. A similar evolution has already been reported during Si buffer growth on holographically patterned Si(001).[11] When the Si buffer layer is increased to 72 nm, the pit morphology is similar, except for a larger pit diameter. An AFM scan of such a pit is shown in Fig. 1(c) and the corresponding "facet plot" is shown in Fig. 1(e), in which each spot corresponds to a particular facet.[17] The pit sidewalls are composed of {113} facets while their corners are decorated by {103} facets. In addition, the continuous intensity distribution in the facet plot indicates the presence of shallower {11*n*} facets and possibly steps at the pit bottoms. When the Si buffer layer is increased to 144 nm, the pits evolve toward inverted truncated pyramids: their diameter increases to ~620 nm while their depth decreases from about 60 to 40 nm. An AFM scan and the corresponding facet plot are shown in Figs. 1(d) and 1(f), respectively. The progressive filling of the pits promotes the expansion of the shallower {11*n*} facets while consuming the steeper {113} and {103} facets. In the following, the Ge deposition on the pit morphology shown in Fig. 1(b) is investigated.

Figure 2 shows AFM scans obtained after deposition of various amounts of Ge at 700 °C on top of a 36 nm thick Si buffer layer. For all Ge coverages considered here (3.75–6 ML) arrays of islands with homogeneous shape are observed only at the pit bottoms, while no islands form between the patterned pits. We obtain a perfect lateral ordering in two dimensions independently on the amount of deposited Ge. If the growth is stopped at 3.75 ML Ge [Fig. 2(a)], a 2D array of TPs is obtained. This is a remarkable result, since on planar Si(001) surfaces TPs are usually observed together

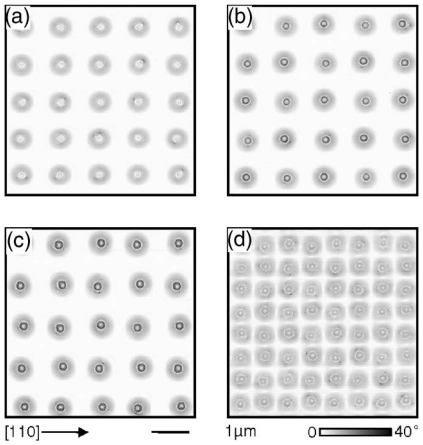

FIG. 2. AFM scans obtained upon deposition of 36 nm Si and subsequent deposition of 3.75 ML Ge (a), 5.0 ML Ge (b), and 6 ML Ge, period 1000 nm (c), and 6 ML Ge, period 600 nm (d) at 700 °C.

with other island shapes (Ps or Ds).[2,18] When the Ge coverage increases further, steeper morphologies appear [Fig. 2(b) and 2(c)]. It is noteworthy that perfectly ordered arrays of SiGe islands can be obtained with pattern periodicities between 600 and 1000 nm [Figs. 2(c) and 2(d)].

Figure 3 shows AFM scans of SiGe islands obtained after deposition of 3.75 ML (a), 4 ML (b), 5 ML (c), 6 ML (d), 7 ML (e), and 8.0 ML (f) Ge at 700 °C. The islands evolve from prepyramids (not shown here) to TPs [Fig. 3(a)] containing a top (001) surface and {105} facets at their side and eventually to mature pyramids bounded by four {105} facets [Fig. 3(b)]. Interestingly, the TD [Fig. 3(c)] appears symmetric while on planar Si(001) surfaces, the TDs follow a series of asymmetric shapes.[19,20] When the Ge coverage increases further, the TDs evolve into Ds bounded by {105}, {113}, and {15 3 23} facets [Fig. 3(d)]. Finally, the latter change their shape and evolve into another transitional structure [Fig. 3(e)] before reaching the barn shape after deposi-

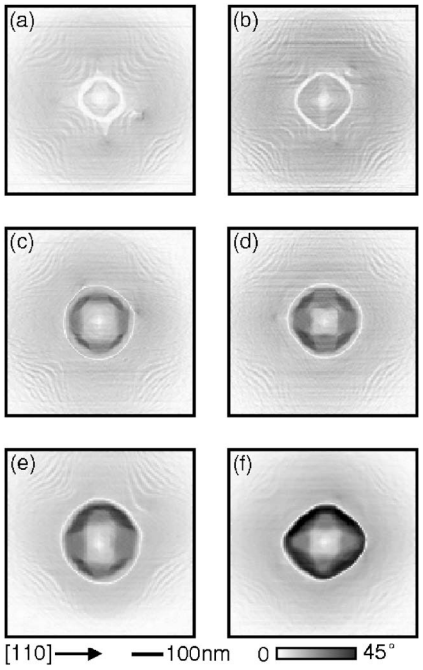

FIG. 3. AFM scans of individual SiGe islands obtained after deposition of 36 nm Si and subsequent deposition of 3.75 ML Ge (a), 4 ML Ge (b), 5 ML Ge (c), 6 ML Ge (d), 7 ML Ge (e), and 8.0 ML Ge at 700 °C (f).

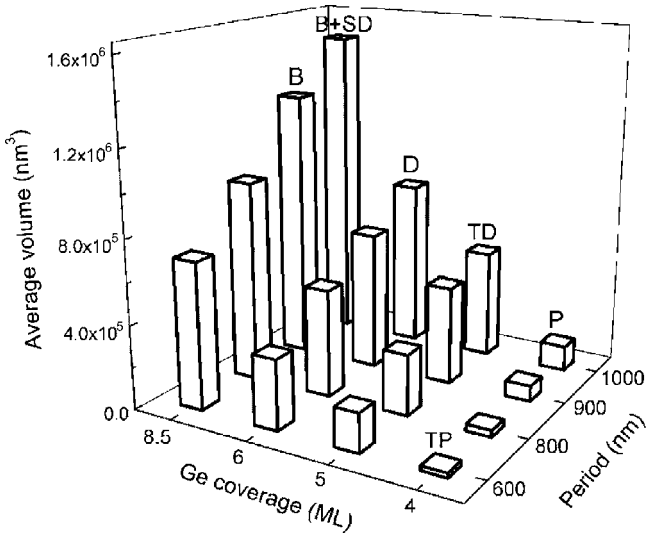

FIG. 4. Average island volume vs Ge coverage and periodicity of the patterned field. Different island types are indicated as TP (truncated pyramid), P (pyramid), TD (transition dome), D (dome), B (barn), and SD (super dome).

tion of 8.0 ML Ge [Fig. 3(f)]. In addition to the dome related facets, steeper {111} as well as {20 4 23} facets are observed at their base. This evolution is similar to that reported recently for SiGe islands on planar Si(001) substrates.[2,16] In contrast to Ref. 21, no new shapes are observed, indicating that the pits employed here do not affect appreciably the equilibrium morphology of the islands.

In order to gain further understanding on the island evolution on patterned substrates, we measured the average island volume as a function of Ge coverage and period of the patterned field (see Fig. 4). At constant Ge coverage and growth temperature, the average island volume increases with the period. Smaller/larger periods lead to the formation of smaller/larger islands. This observation can be easily understood if we assume that each pit represents a local minimum of the chemical potential and therefore the center of a capture zone. The fact that no islands are observed between pits indicates that the migration length of the Ge adatoms is larger than the pit spacing and that all Ge atoms impinging in the capture zone around a pit will contribute to the volume of the corresponding island (plus the surrounding WL). This is supported by the following: if we assume that the WL thickness and the Ge content of SiGe islands are the same on fields with different periods, the average SiGe island volume on the field with period 1000 nm should be by a factor of 2.78 (100/36) larger than the corresponding one on the field with period 600 nm, e.g., for 5 ML Ge coverage, Fig. 4 shows that this ratio is 2.81, which is close to 2.78.

Therefore, the presence of an ordered pattern produces islands with similar sizes, and consequently with similar shapes. On planar substrates, ripening of larger/steeper islands at the expense of smaller/shallower islands[2,22] renders it difficult to produce ensembles of islands with the same shape. The observation of homogeneous arrays of TPs on the patterned substrate indicates that ripening (coarsening) is strongly suppressed with respect to growth on planar substrates. Since coarsening takes place when islands with slightly different sizes are able to exchange material, we conclude that the presence of pits hinders this process. Although the adatom migration length appears to be large enough to allow for material exchange among islands and the probability of adatom detachment from an island is probably not affected by the presence of a pit, the pit does affect the surface diffusion of adatoms away from an island. Since each pit represents a local minimum of the chemical potential, we imagine that adatoms detaching from an island get incorporated again into the same island before possibly moving to other islands and produce coarsening of the ensemble. The large pit depth (about 60 nm) used in our experiment may be responsible for such a behavior. Within the capture zone picture we can also rationalize the observation of symmetric TDs. Asymmetric shapes observed on planar surfaces are attributed to asymmetries in the neighborhood of the islands.[19] Since the shape of the periodically distributed pits after buffer growth has fourfold symmetry, we expect the flux of Ge contributing to island growth to be isotropic and to favor the development of fourfold symmetric structures.

In summary, we have investigated the morphological evolution of both pits during Si buffer growth and SiGe islands during subsequent Ge deposition. Ordered island arrays with large spacing are of paramount importance both for investigations of single islands as well as for their integration in future nanoscale devices.

This work was supported by the EC projects SANDiE and D-DOTFET (Contract Nos. NMP4-CT-2004-500101 and 012150).

[1] J. Stangl, V. Holý, and G. Bauer, Rev. Mod. Phys. **76**, 725 (2004).
[2] A. Rastelli, M. Stoffel, U. Denker, T. Merdzhanova, and O. G. Schmidt, Phys. Status Solidi A **203**, 3506 (2006) and references therein.
[3] O. G. Schmidt and K. Eberl, IEEE Trans. Electron Devices **48**, 1175 (2001).
[4] K. W. Ang, C. H. Tung, N. Balasubramanian, G. S. Samudra, and Y. C. Yeo, IEEE Electron Device Lett. **28**, 609 (2007).
[5] R. A. Donaton, D. Chidambarrao, J. Johnson, P. Chang, Y. Liu, W. K. Henson, J. Holt, X. Li, J. Li, A. Domenicucci, A. Madan, K. Rim, and C. Wann, Tech. Dig. - Int. Electron Devices Meet. **2006**, 465.
[6] *Lateral Alignment of Epitaxial Quantum Dots*, edited by O. G. Schmidt (Springer, Berlin, 2007).
[7] E. S. Kim, N. Usami, and Y. Shiraki, Appl. Phys. Lett. **72**, 1617 (1998).
[8] O. G. Schmidt, N. Y. Jin-Phillipp, C. Lange, U. Denker, K. Eberl, R. Schreiner, H. Gräbeldinger, and H. Schweizer, Appl. Phys. Lett. **77**, 4139 (2000).
[9] Z. Zhong, A. Halilovic, M. Mühlberger, F. Schäffler, and G. Bauer, Appl. Phys. Lett. **82**, 4779 (2003).
[10] C. Dais, H. H. Solak, Y. Ekinci, E. Müller, H. Sigg, and D. Grützmacher, Surf. Sci. **601**, 2787 (2007).
[11] Z. Zhong and G. Bauer, Appl. Phys. Lett. **84**, 1922 (2004).
[12] G. Chen, H. Lichtenberger, G. Bauer, W. Jantsch, and F. Schäffler, Phys. Rev. B **74**, 035302 (2006).
[13] G. Medeiros-Ribeiro, A. M. Bratkovski, T. I. Kamins, D. A. A. Ohlberg, and R. S. Williams, Science **279**, 353 (1998).
[14] I. Goldfarb, P. T. Hayden, J. H. G. Owen, and G. A. D. Briggs, Phys. Rev. Lett. **78**, 3959 (1997).
[15] V. Zela, I. Pietzonka, T. Sass, C. Thelander, S. Jeppesen, and W. Seifert, Physica E (Amsterdam) **13**, 1013 (2002).
[16] M. Stoffel, A. Rastelli, J. Tersoff, T. Merdzhanova, and O. G. Schmidt, Phys. Rev. B **74**, 155326 (2006).
[17] M. A. Lutz, R. M. Feenstra, P. M. Mooney, J. Tersoff, and J. O. Chu, Surf. Sci. **316**, L1075 (1994).
[18] A. Rastelli, H. von Känel, B. J. Spencer, and J. Tersoff, Phys. Rev. B **68**, 115301 (2003).
[19] F. M. Ross, R. M. Tromp, and M. C. Reuter, Science **286**, 1931 (1999).
[20] F. Montalenti, P. Raiteri, D. B. Migas, H. von Känel, A. Rastelli, C. Manzano, G. Costantini, O. G. Schmidt, U. Denker, K. Kern, and L. Miglio, Phys. Rev. Lett. **93**, 216102 (2004).
[21] Z. Zhong, W. Schwinger, F. Schäffler, G. Bauer, G. Vastola, F. Montalenti, and L. Miglio, Phys. Rev. Lett. **98**, 176102 (2007).
[22] F. M. Ross, J. Tersoff, and R. M. Tromp, Phys. Rev. Lett. **80**, 984 (1998).